SUPPLEMENTAL INFORMATION

Immune escape via a transient gene expression program enables productive replication of a latent pathogen

Jessica A. Linderman[#], Mariko Kobayashi[#], Vinayak Rayannavar,
John J. Fak, Robert B. Darnell, Moses V. Chao, Angus C. Wilson, & Ian Mohr

[#] Equal co-first author

Supplemental Information Contents:

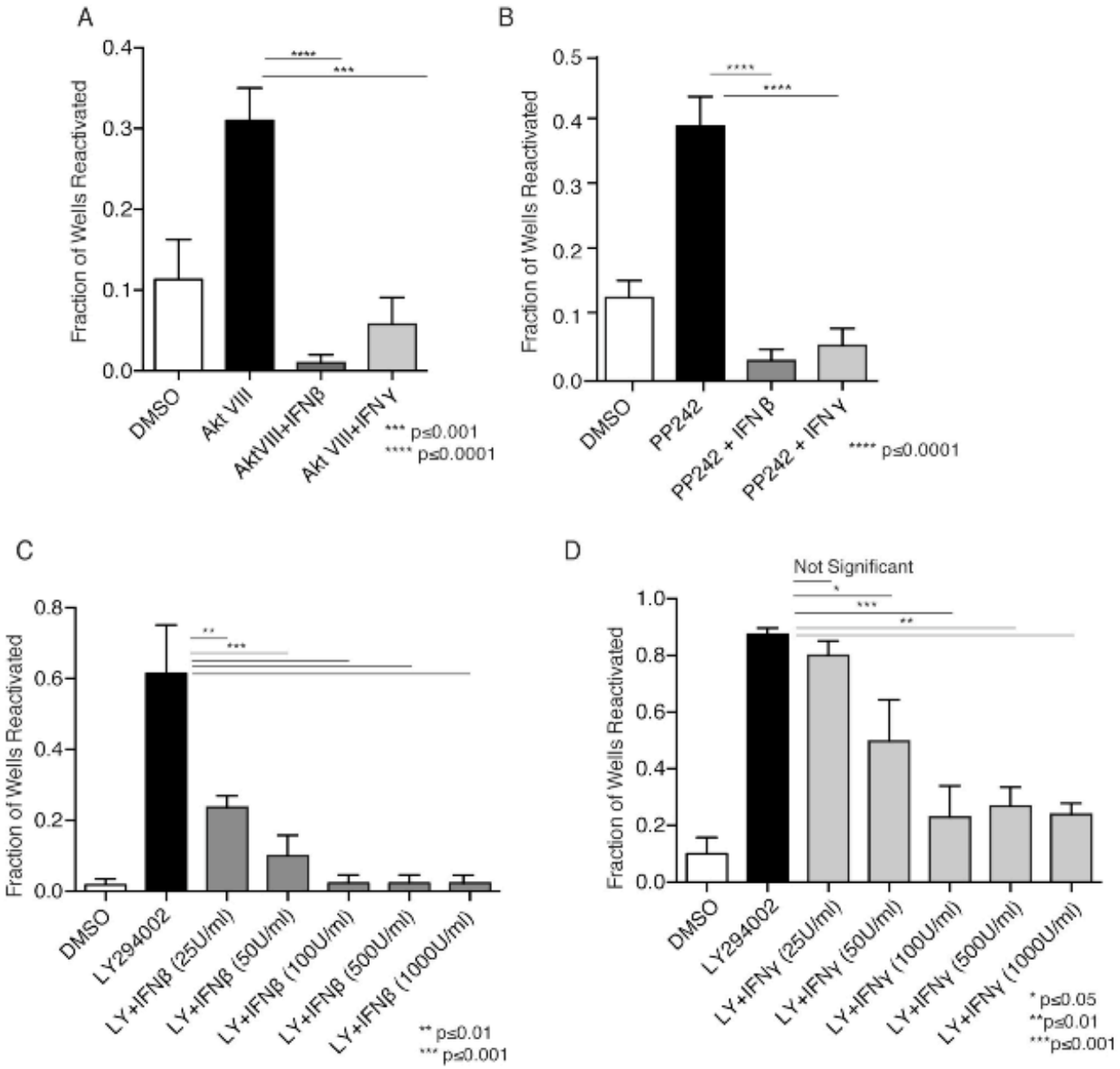

Figure S1. IFN blocks reactivation induced by PI3K, Akt and mTOR inhibitors, related to Figure 1. Neurons were treated with 100 U/ml IFNβ or IFNγ in the presence of (A) Akt Inhibitor VIII (Akt VIII) or (B) the mTOR active-site inhibitor PP242 applied to latently-infected neurons for 20 h. Akt Inhibitor VIII induced reactivation in 31% of wells treated with inhibitor alone, but this was reduced to only 1% by including IFNβ ($p \leq 0.0001$) and 6% with IFNγ ($p \leq 0.001$). Treatment with the mTOR-specific inhibitor PP242 induced reactivation in 39% of wells, which was reduced to 3% ($p \leq 0.0001$) or 6% ($p \leq 0.0001$) by IFNβ and IFNγ, respectively. (C,D) Neurons were pulsed with 20 μM LY294002 and increasing concentrations of (C) IFNβ or (D) IFNγ. After 20h, the media was removed and replaced with fresh media or media containing only IFN. Reactivation was scored 4 days after the initiation of inhibitor treatment as the fraction of EGFP-positive wells.

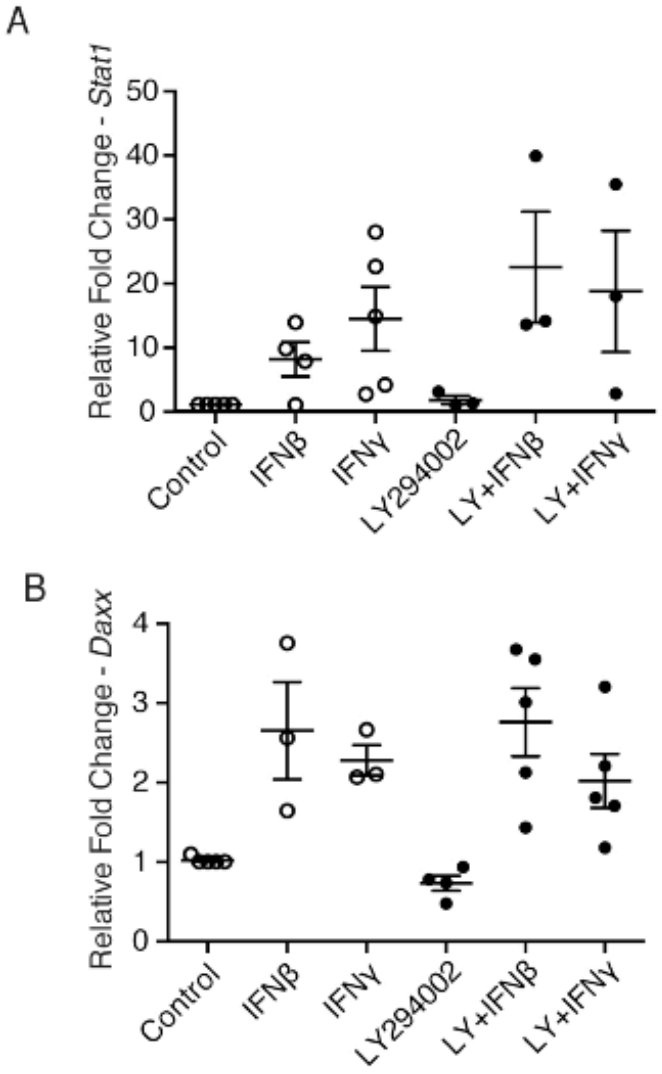

Figure S2. LY-induced reactivation does not detectably interfere with IFN-stimulated DAXX and STAT1 mRNA accumulation in neurons, related to Figure 2. Latently-infected neurons were treated with 20 μM LY alone or with 100 U/ml IFNβ or IFNγ. RNA was collected after 20 h and the levels of mRNA for ISGs Stat1 (A) and Daxx (B) measured by qRT-PCR.

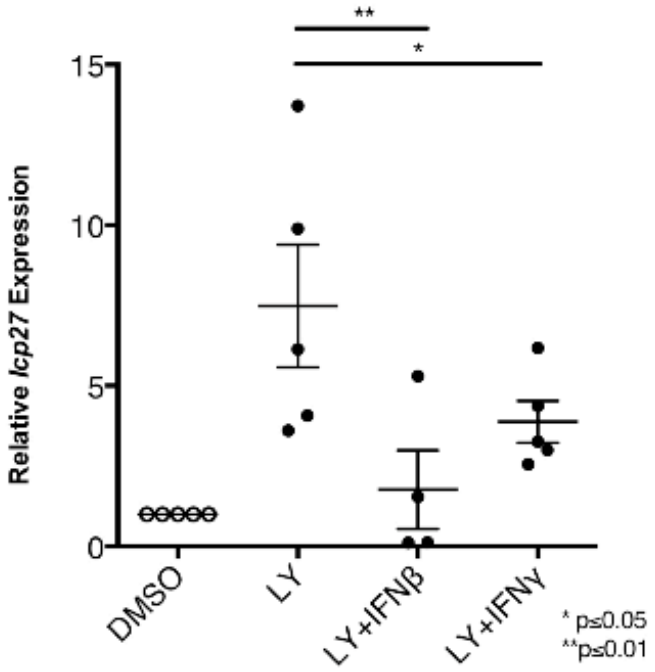

Figure S3. Suppression of HSV1 KOS strain reactivation by IFN, related to Figure 3. Neurons latently-infected with wild-type HSV-1 strain KOS were treated with vehicle only (DMSO) or 20 μM LY294002 alone or in the presence of 100 U/ml IFNβ or IFNγ. After 20 h, mRNA was collected and the accumulation of the HSV-1 ICP27 lytic transcript analyzed by qRT-PCR.

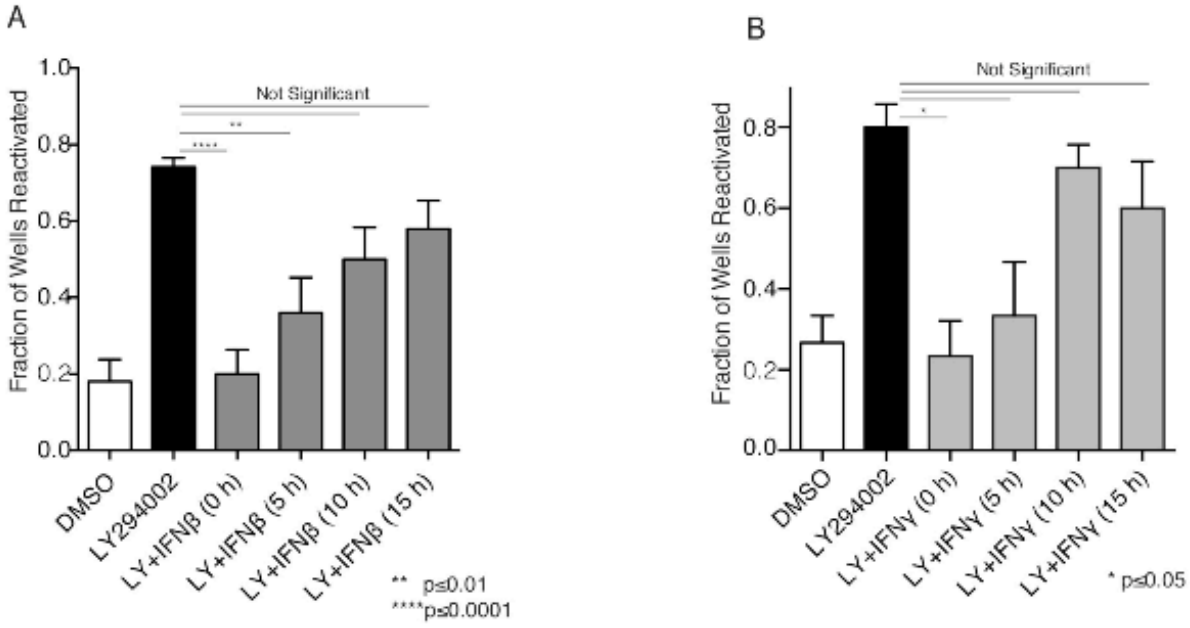

<u>Figure S4</u>. Suppression of reactivation by IFN is limited to a temporal window within Phase I, related to Figure 3. Latently-infected neurons induced to reactivate with LY294002 for 20 h were treated with (A) 100 U/ml IFNβ or (B) 100 U/ml IFNγ at the time of LY addition (*0h*), or at the indicated times after LY application (*5h, 10h, 15 h).* After 20h, the LY was removed and incubation in the presence of IFN continued. Reactivation was scored 4 days after LY294002 addition.

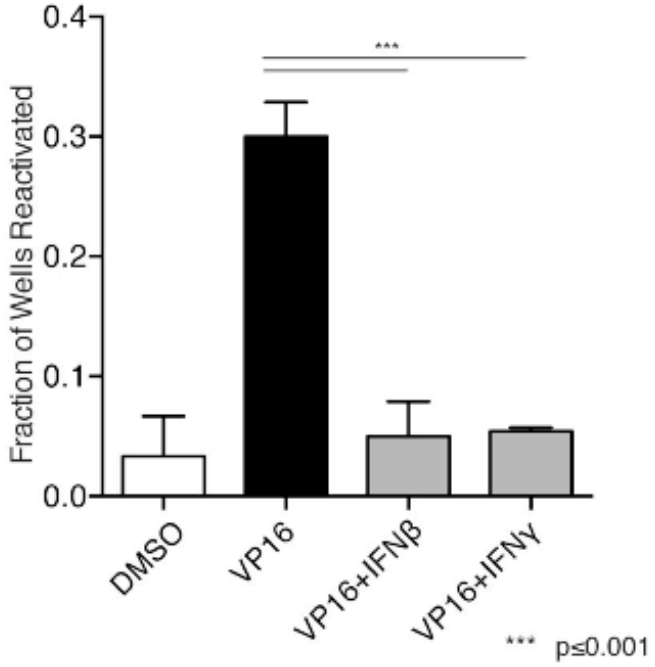

<u>Figure S5</u>. IFNβ and IFNγ can counter HSV-1 reactivation induced by ectopic VP16, related to Figure 5. VP16 was expressed from a doxycycline (dox)-inducible promoter using a recombinant adenovirus vector in neurons latently-infected with HSV-1. The percentage of wells in which HSV-1 had reactivated in the presence or absence of 100 U/ml IFNβ or 100 U/ml IFNγ was scored 4 days after the induction of VP16 expression. DMSO-treated cultures provided a control for spontaneous reactivation in the absence of any inducer.

LIST OF SUPPLEMENTARY TABLES PROVIDED IN EXCEL SPREADSHEET

Table S1. Genes responsive to both IFNβ and IFNγ in neurons induced to reactivate.

Table S2. Genes uniquely responsive to IFNβ in neurons induced to reactivate.

Table S3. Genes uniquely responsive to IFNγ in neurons induced to reactivate.

Table S4. Pathway analysis of genes uniquely induced by IFNβ in neurons induced to reactivate.

Table S5. Pathway analysis of genes uniquely induced by IFNγ in neurons induced to reactivate.

Table S6. Neuronal enriched genes induced by both IFNβ and IFNγ in neurons induced to reactivate.

SUPPLEMENTAL EXPERIMENTAL PROCEDURES

Quantitative reverse transcription PCR analysis. Total RNA was isolated using a modified protocol for the RNeasy Mini Kit (*QIAGEN*). Ten wells of neurons were pooled and lysed in 175 µl of RLT Buffer (*QIAGEN*) and centrifuged through a QIAGEN Shredder for homogenization. Each sample was brought to a total volume of 450 µl with RNase-free water and RNA was precipitated with 450 µl of 100% ethanol. The samples were then applied to the RNeasy columns, washed as per manufacturer's instructions and eluted with RNase-free water. The samples were next DNase I (*New England Biolabs*) treated for 10 min at 37°C to eliminate contaminating DNA and the DNase I was subsequently heat inactivated at 75°C for 10 min in the presence of 2 mM EDTA. cDNA was generated from each sample using qScript (*Fermentas*). Input RNA was normalized using 18S rRNA primers (SA Biosciences) and quantitative real-time PCR (qRT-PCR) analysis performed using iQ-BioRad SYBR Green Supermix (BioRad) and a MyiQ single-color real-time thermal cycler (*BioRad*). Levels of selected viral lytic mRNAs were determined by qRT-PCR using the following primer sets (*Kim et al, 2012)*:

ICP27 FW: 5'-TTTCTCCAGTGCTACCTGAAGG-3'

ICP27 RV: 5'-TCAACTCGCAGACACGACTCG-39'

UL30 FW: 5'-CGCGCTTGGCGGGTATTAACAT-3'

UL30 RV: 5'-TGGGTGTCCGGCAGAATAAAGC-3'

Relative mRNA transcript levels were calculated using the ddCt method and data plots and statistical calculations were made using Prism 5.0 software (*GraphPad*).

Immunoblotting and Antibodies. Total protein was collected by lysis in Laemmli buffer from 20 pooled wells and fractionated on SDS-polyacrylamide gels of either 10% (STAT1 and DAXX) or 17.5% (4E-BP1). The protein was then transferred onto nitrocellulose membranes, blocked with 5% milk in TBS-T for 30 min and incubated overnight at 4°C with antibodies against STAT1 (C*ell Signaling*, #9172), DAXX (*Cell Signaling*, #4533), 4E-BP1 (*Bethyl*, #A300-501A) or ! -tubulin (*Sigma*, #T9026*)*. Primary antibodies were detected using either anti-mouse IgG HRP (*GE Healthcare*, #NA931V) or anti-rabbit IgG HRP (*Sigma Aldrich*, #A0545) secondary antibodies and visualized by chemiluminescent detection.

Reactivation by expression of mutant 4EBP1. Reactivation was induced by the expression of an HA-epitope-tagged T37A/T46A 4E-BP1 double mutant (AA) as previously described (*Kobayashi et al., 2012*). The mutant was delivered into neurons using a lentiviral vector packaged in 293LTV cells by cotransfection of the vector plasmid together with the " 8.9 (gag-pol-rev) and pMDG.2 (VSV envelope) packaging plasmids. Latently-infected neurons were transduced with infectious lentiviral particles on Day 12 *in vitro* (6 days after HSV-1 infection). Media containing ACV and lentivirus was removed the next day and replaced with media containing or lacking doxycycline (dox) and 100 U/ml IFN. Two days later, mRNA was prepared and analyzed by qRT-PCR as described below.

Adenoviral expression. ICP0 and VP16 were ectopically delivered and expressed independent of HSV-1 using a recombinant adenovirus vector (Ad.T-ICP0; Ad.T.VP16) under the direction of a tetracycline-responsive promoter (*Halford & Schaffer, 2001*). Neurons were coinfected with a mixture of Ad.T-ICP0 or Ad.T-VP16 (MOI = 40) and Ad.C-rtTA (MOI = 10) that constitutively expresses the reverse tetracycline-regulated transactivator (rtTA). Following exposure to fresh media containing the adenoviruses for 1 h to allow viral adsorption, neuron cultures were refed with media containing 3 μM doxycycline, a tetracycline analog, in the absence or presence of IFNβ or γ.

RNA-seq data analysis. Sequencing reads were aligned using the STAR aligner (v2.5.0a) to the Rnor 6.0 genome (*Dobin et al., 2013*). Ensembl Rnor 6.0 annotation was used to create the splice junction database to guide the alignment, and later to quantify reads per gene. featureCounts v1.4.3-p1 was used for read quantification (*Liao et al., 2014*). Analysis of RNA-seq defined gene expression changes in IFN treatments was carried out in R (www.r-project.org; [Ihaka and Gentleman, 1996]) using Bioconductor (*Gentleman et al., 2004*) and the package edgeR (*Robinson and Oshlack, 2010*) applying generalized linear model methods to account for biological variation across replicates (*McCarthy et al., 2012*). Expressed genes were defined by having a total sum greater than 200 RNA-seq tags across biological replicates and conditions of pairwise comparison. After filtering out lowly expressed genes, 11,187 and 11,081 genes were used for comparison in LY alone *vs* LY + IFNβ,

and in LY alone *vs* LY + IFNγ, respectively.

Analysis of differentially expressed genes in response to IFNs. Clustered heatmap of log_2 fold change values of differentially expressed genes (responding to either IFNβ or IFNγ) was generated using package pheatmap using the hclust method for clustering (*Kolde, 2015*). Venn Diagram depicting overlap of IFNβ and IFNγ specific genes was made using VennDiagram (*Chen and Boutros, 2011*), statistical significance of overlap between the gene lists calculated by hypergeometric testing. To perform functional enrichment analysis, we used Ingenuity Pathway Analysis (Ingenuity Systems; www.ingenuity.com, Qiagen Bioinformatics), which assesses statistical significance using right-tailed Fisher exact test to calculate a P value determining the probability that each biological function assigned to that dataset is caused by chance alone. Cell-type specific RNAseq fold enrichment values were calculated using metrics previously defined, orthologous gene IDs converted from mouse to rat, and assigned to IFN induced genes identified in this study (*Cahoy et al., 2008, Zhang et al., 2014*). pheatmap was used to generate a heatmap of top 10 neuron enriched, IFN responsive genes. Oligodendrocyte values represent data associated with myelinating oligodendrocytes only.

SUPPLEMENTAL REFERENCES

Cahoy, J.D., Emery, B., Kaushal, A., Foo, L.C., Zamanian, J.L., Christopherson, K.S., Xing, Y., Lubischer, J.L., Krieg, P.A., Krupenko, S.A., et al. (2008). A transcriptome database for astrocytes, neurons, and oligodendrocytes: a new resource for understanding brain development and function. J. Neurosci. *28,* 264-278.

Chen, H., and Boutros, P.C. (2011). VennDiagram: a package for the generation of highly-customizable venn and euler diagrams in r. BMC Bioinformatics *12*, 35.

Dobin, A., Davis, C.A., Schlesinger, F., Drenkow, J., Zaleski, C., Jha, S., Batut, P., Chaisson, M., and Gingeras, T.R. (2013). STAR: ultrafast universal RNA-seq aligner. Bioinformatics. *29*, 15-21.

Gentleman, R.C., Carey, V.J., Bates, D.M., Bolstad, B., Dettling, M., Dudoit, S., Ellis, B., Gautier, L., Ge, Y., Gentry, J. et al. (2004). Bioconductor: open software development for computational biology and bioinformatics. Genome Biol. *5*, R80.

Halford, W.P., and Schaffer, P.A. (2001). ICP0 is required for efficient reactivation of herpes simplex virus type 1 from neuronal latency. J. Virol. *75*, 3240-3249.

Ihaka, R., and Gentleman, R. R. (1996). A language for data analysis and graphics. J.Comp. and Graph. Stat. *5*, 299-314.

Kim, J.Y., Mandarino, A., Chao, M.V., Mohr, I., and Wilson, A.C. (2012). Transient reversal of episome silencing precedes VP16-dependent transcription during reactivation of latent HSV-1 in neurons. PLoS Pathog. *8*, e1002540.

Kobayashi, M., Wilson, A.C., Chao, M.V., and Mohr, I. (2012). Control of viral latency in neurons by axonal mTOR signaling and the 4E-BP translation repressor. Genes Dev. *26*, 1527-1532.

Liao, Y., Smyth, G.K. and Shi, W. (2014). featureCounts: an efficient general purpose program for assigning sequence reads to genomic features. Bioinformatic*s 30*, 923-930.

McCarthy, D.J., Chen, Y., Smyth, G.K. (2012). Differential expression analysis of multifactor RNA-Seq experiments with respect to biological variation. Nuc. Acids Res. *40*, 4288-4297.

Kolde, R. (2015). pheatmap: Pretty Heatmaps. R package version 1.0.8. http://CRAN.R-project.org/package=pheatmap

Robinson, M.D., and Oshlack, A. (2010). A scaling normalization method for differential expression analysis of RNA-seq data. Genome Biol. *11,* R25.

Zhang, Y., Chen, K., Sloan, S.A., Bennett, M.L., Scholze, A.R., O'Keeffe, S., Phatnani, H.P., Guarnieri, P., Caneda, C., Ruderisch, N.. et al. (2014). An RNA-sequencing transcriptome and splicing database of glia, neurons, and vascular cells of the cerebral cortex. J. Neurosci. *34*, 11929-119247.